

Quasikinematic low-energy electron-diffraction surface crystallography

J. F. Jia, R. G. Zhao, and W. S. Yang

Department of Physics, Peking University, Beijing 100871, China

(Received 5 March 1993)

Based on the idea of constant-momentum-transfer averaging (CMTA) of Lagally *et al.* and facing the problem of CMTA pointed out by Pendry, in the present work we propose the use of the quasikinematic low-energy electron-diffraction (QKLEED) calculations in comparison with the experimental CMTA curves in surface structure determinations. In QKLEED, the influences of the zero-angle scattering on the CMTA curves are treated so that they have essentially no influence on correctly determining the structural parameters, and the mean complex atomic scattering factors are introduced as the effective scattering factors. In addition, an experimental design is proposed for obtaining CMTA curves containing the least influence of multiple scattering. The whole QKLEED/CMTA method has been carefully and systematically tested, and its capability of determining surface structures is demonstrated on the Cu(001)(1 × 1), Si(111)($\sqrt{3} \times \sqrt{3}$)R 30°-Al, and Si(111)($\sqrt{3} \times \sqrt{3}$)R 30°-Ag surfaces.

I. INTRODUCTION

It is known that low-energy electron diffraction (LEED) is very well established both theoretically and experimentally¹⁻⁴ and it has been the most important technique for surface structure determinations ever since the late 1960s,⁵ when surface crystallography had just emerged. Unfortunately, it is also known that the full dynamical LEED (DLEED) calculations are very time consuming, especially when complex structures are studied. Consequently, most of the development of LEED theory has concentrated upon ways of reducing the computational requirements through the use of approximations to full multiple scattering as well as symmetries in real and reciprocal spaces. As a result, a tour-de-force analysis of the most complex surface structure Si(111)-(7 × 7) was performed recently by Tong *et al.*⁶ However, the *r* factor of their best-fit structure is by no means small enough to eclipse other models with confidence.

On the other hand, kinematic LEED (KLEED) calculations are much simpler and thus faster. Unfortunately, they do not describe the process of low-energy electron diffraction in most real crystals with an accuracy.^{1,4} In order to take advantage of computational simplicity of KLEED calculations, Lagally, Ngoc, and Webb proposed the method of constant-momentum-transfer averaging (CMTA) to extract from experimental curves the essentially kinematic component.⁷ Many efforts have been devoted to testing, applying, and improving the method,⁸⁻²⁹ especially in the first five years of the method. Some of them ended with satisfactory results^{12,19} while some others failed, especially those involving overlayer structures.^{14,26}

Actually, right after the CMTA method was proposed, Pendry analyzed it and pointed out that⁹ (i) a true kinematic average is impossible; (ii) in CMTA curves the residual influences of multiple scattering are mainly from zero-angle scattering with the result that CMTA curves compared to true kinematic ones have generally lowered (raised) inner potential, reduced intensities, and increased

peak widths; (iii) CMTA curves have a quasi-kinematic form with nonstructural parameters different from those of the true kinematic ones. In addition, Pendry also pointed out that a simple way of calculating effective scattering factors must be developed so that CMTA can be applied with confidence to structural determinations.⁹

From the viewpoint of surface crystallography, one really does not care very much if the nonstructural parameters are influenced by the residual effects of multiple scattering; all that is of interest is an effective and reliable method of determining geometric parameters. Nevertheless, to have the right nonstructural parameters is not a matter that can be completely neglected in structural determinations. In view of these considerations, in the present paper we have proposed a method which allows us to sidestep those complicated influences of multiple scattering on nonstructural parameters while getting good quasikinematic fits to the CMTA curves, and obtain a simple way of calculating the effective scattering factors to be used in the fitting. In addition, an effective way of obtaining the best CMTA curves is proposed and a very efficient scheme of parameter optimization is adopted. The correctness and effectiveness of the methods proposed in this work have been carefully tested and are discussed. Finally, the methods are used in the structural determination of the Si(111)($\sqrt{3} \times \sqrt{3}$)R 30°-Al surface.

II. QUASIKINEMATIC LEED (QKLEED) APPROACH

To fit their CMTA curves, assuming a uniform attenuation of the elastic beam and a scattering factor the same for all atoms, Lagally and co-workers^{7,8,12} calculated the quasikinematic intensities using

$$I(S) = \{|f(\theta, E)|^2\} e^{-2M} L(\mathbf{k}) [1 - W(S)]^2 F(S), \quad (1)$$

where $\{|f(\theta, E)|^2\}$ is the averaged atomic scattering factor, or effective atomic scattering factor, e^{-2M} is the Debye-Waller factor, $L(k)$ is the Lorentz factor, $[1 - W(S)]^2$ is a correction for the surface losses, and the

interference function is

$$F(S) = \sum_{ij} a_i a_j \exp[i\mathbf{S} \cdot (\mathbf{r}_i - \mathbf{r}_j)], \quad (2)$$

where the momentum transfer $\mathbf{S} = \mathbf{k} - \mathbf{k}_0$, \mathbf{k} and \mathbf{k}_0 are the wave vectors of the scattered and incident beams, \mathbf{r}_i is the position of the i th atom, and a_i is the relative contribution of the i th atom. Assuming that the ratio of the amplitudes contributed to the diffracted beam by atoms in successively deeper planes is a constant $\alpha = A_{n+1}/A_n$, then $a_i = \alpha^{n_i}$, where n_i specifies the plane containing the i th atom.

In the present work, the following improvements have been made.³⁰

(i) The Debye-Waller factor, Lorentz factor, and surface loss all cause the intensity to slowly decrease with the beam energy, and now, according to Pendry,⁹ the zero-angle scattering makes the CMTA intensities slowly decrease further. Consequently, we describe the effect of all these factors with a damping factor $E^{-\alpha}$, where α is a parameter to be optimized.

(ii) Since the zero-angle scattering modifies the inner potential,⁹ as a first-order approximation, we treat the inner potential as a parameter to be optimized.

(iii) We describe the effect of inelastic scattering by means of the mean free path λ of the incident electrons, which is also treated as a parameter to be optimized.

(iv) The zero-angle scattering also increases the widths of peaks of CMTA curves⁹ and its effect may be taken into account with the variable mean free path. However, it seems better to treat it separately, since the mean free path also determines the relative contributions of the surface and bulk regions. Therefore, we introduce a broadening factor into our work. To be specific, we replace the intensity at any given energy point by a Lorentzian curve which has a limited width and sum up all these curves to get the quasikinematic intensity

$$I_n(E) = \sum_{n=-3}^3 C_n(w) I(E + n\delta E) / \sum_{n=-3}^3 C_n(w), \quad (3)$$

where

$$C_n(w) = w^2 / \{w^2 + [S_{\perp}(E) - S_{\perp}(E + n\delta E)]^2\}, \quad (4)$$

where w is the broadening factor, a parameter to be optimized, δE is the interval between two neighboring energy points, and S_{\perp} is the momentum transfer perpendicular to the surface. Equation (3) reflects the fact that the Bragg peaks have the same width in S_{\perp} coordinate. For the surfaces tested in this work, w is around 0.24 \AA^{-1} ; in other words, a δ function of intensity is broadened into a peak with a full width at half maximum of 8–10 eV in energy coordinate.

(v) Although Ngoc, Lagally, and Webb have shown that if the surface consists of the same atoms the effective scattering factor equals fairly well to the averaged atomic scattering factor,¹² very often the surface under investigation consists of more than one type of atom. Here we propose a simple way of calculating the effective scattering factor, which can be applied to any surfaces. As the amplitude and phase of the scattered wave are deter-

mined by the modulus and phase angle of the atomic scattering factor of the scattering atom, respectively, no matter what kind of method is to be used, the information provided by the phase angle of a scattering atom should not be discarded especially when the surface consists of more than one type of atom. In view of the average character of CMTA, we propose the use of the mean complex atomic scattering factor (MCASF), which is a mean over the same incidence geometries as in CMTA. To calculate the MCASF of an atom, which corresponds to a diffraction beam, we first calculate a set of atomic scattering factors from the phase shifts of the atom, which have the same incidence geometries as those of the CMTA curve of the beam. The formula is

$$f(\theta, E) = (1/k) \sum_l (2l+1) \exp(i\delta_l) \sin\delta_l P_l(\cos\theta), \quad (5)$$

where δ_l is the phase shift at the energy of E , \mathbf{k} is the incidence wave vector, $P_l(\cos\theta)$ is the Legendre polynomials, and θ is the scattering angle. Then we calculate the MCASF $f_{i,gh}(S_{\perp})$, which is involved in scattering by the i th atom to the diffraction beam (g, h), by averaging the set of atomic scattering factors in the same way as in CMTA. It should be pointed out that such MCASF's are different for different atomic species, diffraction beams, and surface symmetries, but are independent of the concrete structure of the unit cell, so that we need to calculate them only once in the process of determining a surface structure.

After the above-mentioned improvements, the quasikinematic intensity of the beam (g, h) is

$$I_{gh}(S_{\perp}) = \left| \sum_i \{f_{i,gh}(S_{\perp})\} \exp(-z_i/\lambda) \times \exp(i\mathbf{S} \cdot \mathbf{R}_i) \right|_{S_{\perp}}^2, \quad (6)$$

where z_i and \mathbf{R}_i are the perpendicular distance from the surface and position vectors of the i th atom, respectively, λ is the mean free path, and α is the attenuation factor. Actually, to facilitate optimizing the inner potential V_0 , it would be better to utilize the I-E form, instead of $I-S_{\perp}$. So, usually, we transform Eq. (6) into

$$I_{gh}(E) = \left| \sum_i \{f_{i,gh}(E)\} \exp(-z_i/\lambda) \times \exp(i\mathbf{S} \cdot \mathbf{R}_i) \right|_E^2, \quad (7)$$

with the incidence angle θ set to any value, normally 0° . Note that $f_{i,gh}(E)$ should take the value of $f_{i,gh}(S_{\perp})$ with S_{\perp} corresponding to E , and E should include the inner potential V_0 . Of course, the CMTA curves should also be transformed into the I-E form with θ set to the same value. Also note that to get the CMTA curves, one needs to set V_0 to a given value. Although after transforming those curves to the I-E form, that value of V_0 is subtracted from E , the influence of the given V_0 still exists, of course, implicitly. However, our results show that such CMTA I-E curves can be used for optimizing V_0 , provided that the optimized V_0 is not too different from the

given V_0 . Before being compared with the CMTA I-E curves, the quasikinematic intensities calculated with (7) have to be broadened with (3). Later on we shall show the validity of the QKLEED method.

III. EXPERIMENTAL DESIGN OF CMTA

Although influence of the zero-angle scattering could never be eliminated from CMTA curves,⁹ contributions of multiple scattering from other sources can be largely reduced.^{7,8} Clearly, the larger the number of the I-E spectra involved in a CMTA curve, the wider the area in the $\theta\phi$ (incidence and azimuth angles) space occupied by the incidence geometries, i.e., (θ, ϕ) 's of the I-E spectra, and the more randomly the (θ, ϕ) 's distribute in the $\theta\phi$ space, the more the influence of multiple scattering is eliminated from the CMTA curve. Consequently, we pay special attention to the following points:³⁰

(i) Throughout our CMTA work we have been using a conventional LEED optics from Riber. The maximum range of θ is 0° – 21° and that of ϕ is 0° – 360° . Using the Ewald sphere, it is not difficult to see that in most cases these ranges are large enough to effectively reduce influences of multiple scattering.³⁰ However, the symmetry of the surface may substantially reduce the effective range of ϕ . For instance, if the surface has a $4m$ symmetry, then for the (0,0) beam the effective range of ϕ is only 0° – 45° , which is probably somewhat too small to effectively eliminate multiple scattering. Such an influence can be clearly seen on the CMTA curve of the (0,0) beam of the Cu(001)(1×1) surface (see Sec. V A). To fully take advantage of the LEED optics to make the (θ, ϕ) 's occupy as large an area as possible in the $\theta\phi$ space and also to give the I-E spectra as wide an energy range as possible, very often we need to measure the degenerated beam, instead of the beam itself.

(ii) It is extremely important to distribute the (θ, ϕ) 's in the $\theta\phi$ space as randomly or evenly as possible, i.e., there should be no correlation between the θ 's and ϕ 's. This has been neglected in many of the previous papers on CMTA.

(iii) Although we have mentioned that the larger the number of the I-E spectra involved in a CMTA curve the better, on the other hand, collecting more spectra than needed is a waste of time. Actually, we have demonstrated through testing that the residual influence of multiple scattering in the CMTA of some 5–10 I-E spectra can be negligible provided the (θ, ϕ) 's are carefully arranged as suggested above.

To see if following the three points just mentioned above can really let us obtain good CMTA curves, i.e., curves containing the least contribution of multiple scattering, we have done a great deal of experimental testing. The results are always positive. The idea of the tests is that if two independent CMTA curves of a diffraction beam match one another, i.e., their R_{vht} (Ref. 31) is smaller than 0.1, then we say both are good. Such tests have been routine in all of our CMTA works. In fact, all CMTA curves of more than 100 beams belonging to some ten different surface structures have tested good, except for a few from very dim fractional-order or, some-

times, from (0,0) beams.³⁰ Some of the tested surfaces are Cu(001)-(1×1), Si(111)($\sqrt{3} \times \sqrt{3}$) $R 30^\circ$ -Al, Si(111)($\sqrt{3} \times \sqrt{3}$) $R 30^\circ$ -Ag, Si(11)(7×7), and Pd(001)(2×2)-Mn. An example of the good agreement between two independent CMTA curves collected from the same beam using the above-mentioned method, is given in Fig. 1, whose R_{vht} is of the average level of our tests.

IV. MODEL TESTS OF THE QKLEED/CMTA METHOD

Two types of tests, namely, the model and application test,³⁰ have been carried out to check the general validity of the QKLEED/CMTA method proposed in the preceding sections.

In a model test of the QKLEED/CMTA, we first calculate from a given surface structure a set of DLEED I-E spectra of a beam, which have their (θ, ϕ) 's arranged in the same manner as that in the experimental CMTA. Second, we average these spectra to get a theoretical CMTA curve. Then, from the same surface structure, we calculate the quasikinematic spectrum of the same beam with the QKLEED. Finally, we compare the theoretical CMTA curve with its quasikinematic counterpart. If they match each other well, then, clearly, it proves the validity of the whole QKLEED/CMTA method. Four different model surfaces have been tested.³⁰ The DLEED programs and phase shifts were essentially from Van Hove and Tong.² The tested surfaces are as follows.

(i) Cu(001)(1×1), with its layer spacings being the same as those determined by Davis and Noonan.³² Since it is a simple metal surface consisting of the same atoms, in the QKLEED calculations we simply assume MCASF's $\equiv 1$. It worked very well, as we have shown previously.²⁹ The total R_{vht} (Ref. 31) of the five beams is 0.12.

(ii) GaP(111)(1×1), with its first layer being Ga atoms and bulklike structure. Since it consists of two different atoms with quite different atomic numbers, in the QKLEED calculations, for both Ga and P atoms we must use their own MCASF's. The total R_{vht} of the six beams is 0.12, while nine I-E spectra are involved in each

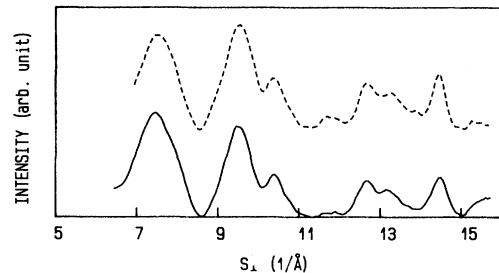


FIG. 1. Comparison of two CMTA curves collected from two degenerated beams, i.e., (0,1) and (1,-1) of the Si(111)($\sqrt{3} \times \sqrt{3}$) $R 30^\circ$ -Ag surface. The R_{vht} of the agreement between the curves is 0.10. The (θ, ϕ) 's (see text) of the (0,1) curve (solid) are $(0^\circ, 0^\circ)$, $(3^\circ, 25^\circ)$, $(6^\circ, -20^\circ)$, $(9^\circ, -65^\circ)$, and $(12^\circ, -105^\circ)$; those of the (1,-1) curve (dashed) are $(0^\circ, 0^\circ)$, $(3^\circ, -70^\circ)$, $(6^\circ, -100^\circ)$, $(9^\circ, -130^\circ)$, $(12^\circ, 170^\circ)$, $(15^\circ, -160^\circ)$, and $(18^\circ, 140^\circ)$.

CMTA curve. However, if only the moduli, i.e., the absolute values, of the MCASF's are used, then the total R_{vht} is 0.34. This shows that the use of MCASF's is not only correct but also very important.

(iii) $\text{NiSi}_2(111)(1 \times 1)$, with its structural parameters being the same as those determined by Yang, Jona, and Marcus with DLEED.³³ This is a real and very condensed structure. The total R_{vht} of the six beams is 0.16, while 11 I-E spectra are involved in each CMTA curve. The slightly poorer r factor is probably due to the fact that the surface is very condensed.

(iv) $\text{Cu}(001)(1 \times 1)\text{-O}$, which is simply a bulklike structure with its first layer replaced by oxygen atoms. Earlier work concluded that CMTA does not work for such surfaces.¹⁴ The total R_{vht} of the five beams is 0.13, while 12 I-E spectra are involved in each CMTA curve. The small r factor indicates that the QKLEED/CMTA method also works for overlayer structures.

In Fig. 2 the results of the $\text{GaP}(111)\text{-}(1 \times 1)$ surface are shown as an example of our model tests.

V. APPLICATION TESTS OF THE QKLEED/CMTA

As we have seen from the model tests, the QKLEED/CMTA method works quite well for a wide range of surface structures. In this section we show the ability of the method to find out the right structural parameters of unknown surface structures. The surfaces tested so far³⁰ are $\text{Cu}(001)(1 \times 1)$, $\text{Si}(111)(\sqrt{3} \times \sqrt{3})R 30^\circ\text{-Al}$, and $\text{Si}(111)(\sqrt{3} \times \sqrt{3})R 30^\circ\text{-Ag}$.

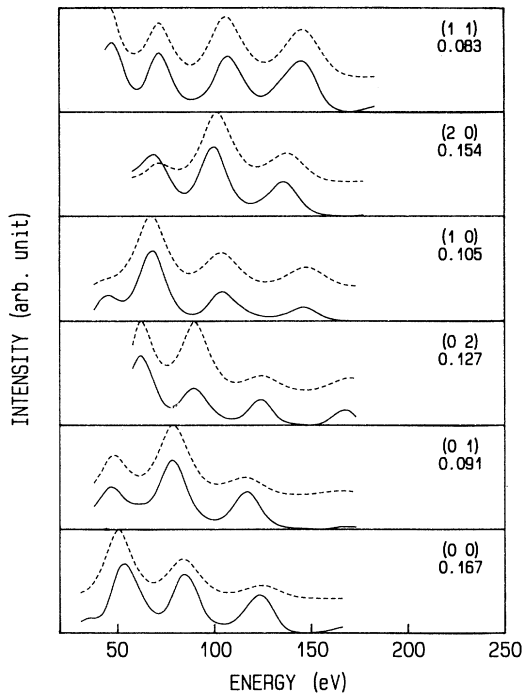


FIG. 2. Comparison of the quasikinematic spectra (dashed) calculated by the QKLEED approach (see text) with the theoretical CMTA curves (solid, see text) of an ideal $\text{GaP}(111)\text{-}(1 \times 1)$ surface. The index and R_{vht} of each beam are shown in the boxes and the total R_{vht} is 0.12.

A. Test with $\text{Cu}(001)(1 \times 1)$

We choose this surface as the first candidate for the tests as its structure has been determined with DLEED,³² while old CMTA analysis^{13,16} of the surface failed (see discussion in Sec. VI). Five experimental CMTA curves were collected³⁰ in the way mentioned above. Again in the QKLEED calculations we assume $\text{MCASF's} \equiv 1$. Starting from the bulklike structure, the searching (see discussion in Sec. VI) resulted in the layer spacings listed in Table I. The results are in excellent agreement with those of DLEED.³² The optimized inner potential is 10.5 eV and the mean free path is 3.8 Å. The QKLEED and CMTA curves, together with their beam index and r factors, are shown in Fig. 3. The total R_{vht} of the five beams is 0.13. As one can see, the residual peaks from multiple scattering are indeed very small except for the (0,0) beam. However, it seems those small residual peaks are not an obstacle to reaching the right surface structure.

B. Test with $\text{Si}(111)(\sqrt{3} \times \sqrt{3})R 30^\circ\text{-Al}$

Ever since the first report of the $\text{Si}(111)(\sqrt{3} \times \sqrt{3})R 30^\circ\text{-Al}$ surface in 1964,³⁴ a great deal of effort has been made to solve the surface structure. Only recently, the model proposed by Northrup,³⁵ which suggests that the Al atoms occupy the T_4 positions (T_4 model), has been receiving more and more support.^{36,37} Since the structure of this surface has been determined by DLEED,³⁸ and it is also quite complex, we choose it as our second candidate for testing the QKLEED/CMTA method. In the experiment CMTA curves of ten beams were collected.³⁰ Each of the CMTA curves involves five or more I-E spectra. In QKLEED calculations for the Si and Al atoms their own MCASF's were used. However, if only the MCASF's of Si are used, no significant difference can be seen, just as in the case of DLEED.³⁸ Starting from any different structures of the T_4 model such as that of Northrup³⁵ and the bulklike structure and some others, optimization resulted in structures very close to one another with the maximum difference of all structural parameters less than 0.03 Å. In Fig. 4 we show the optimized structure of this work as well as that of DLEED.³⁸ The agreement between the two structures is excellent. The QKLEED curves and their experimental CMTA counterparts are shown in Fig. 5. The total R_{vht} of the ten beams is 0.158. The optimized inner potential is 11.8 eV and the mean free path is 6.0 Å. For all bonds in our optimized structure, the bond length deviation from the bulk value is smaller than 5%, indicating clearly the correctness of the structure. We have also tried to optimize the H_3 model, in which the Al atoms occupy the H_3 positions, but the lowest total R_{vht} of the model that we could reach was 0.21.

C. Test with $\text{Si}(111)(\sqrt{3} \times \sqrt{3})R 30^\circ\text{-Ag}$

Except for the $\text{Si}(111)(7 \times 7)$, this surface has probably been the most studied one and it is still a controversial issue.³⁹⁻⁴² To make sure the QKLEED/CMTA method can be effectively used to determine structure of surfaces consisting of atoms with very different atomic numbers,

TABLE I. Relaxation (relative to the bulk value of 1.808 Å) of the first four layer spacings of the Cu(001)(1×1) surface determined with QKLEED/CMTA and DLEED.

	First	Second	Third	Fourth
QKLEED/CMTA	-1.3%	+1.7%	+1.1%	+1.1%
DLEED (Ref. 32)	-1.1±.4%	+1.7%±.6%	≥1.0%	

we employed it to determine the Si(111)($\sqrt{3}\times\sqrt{3}$)R30°-Ag surface and wound up with a structure which is in excellent agreement with most recent results⁴⁰⁻⁴² and whose total R_{vht} of all ten beams is 0.16.³⁰ The details will be published elsewhere.⁴³

VI. DISCUSSIONS

A. Convergence of the MCASF

We have seen that any two independent CMTA curves of the same beam can be very similar even if each involves only 5-10 I-E spectra, provided that the (θ, ϕ) 's of these spectra are carefully arranged in the manner discussed in Sec. III. In other words, such CMTA curves have convergence. To make the QKLEED curves compatible with such CMTA curves, the MCASF's used in

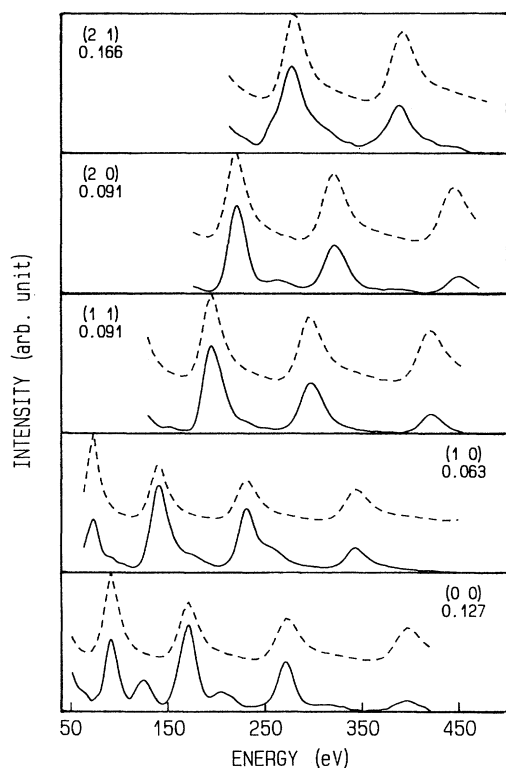


FIG. 3. Comparison of the QKLEED curves (dashed) with the CMTA curves (solid) of the Cu(001)(1×1) surface. The structural parameters of the surface are listed in Table I. The beam indices and r factors are shown in the boxes. The total R_{vht} of the five beams is 0.13.

the QKLEED calculations should also have convergence. To verify this, we have tested the influence of the number and (θ, ϕ) 's of the I-E spectra involved on the resulting MCASF's. It turns out that the MCASF's indeed converge even if the number of the spectra is only ten or less. An example is shown in Fig. 6.

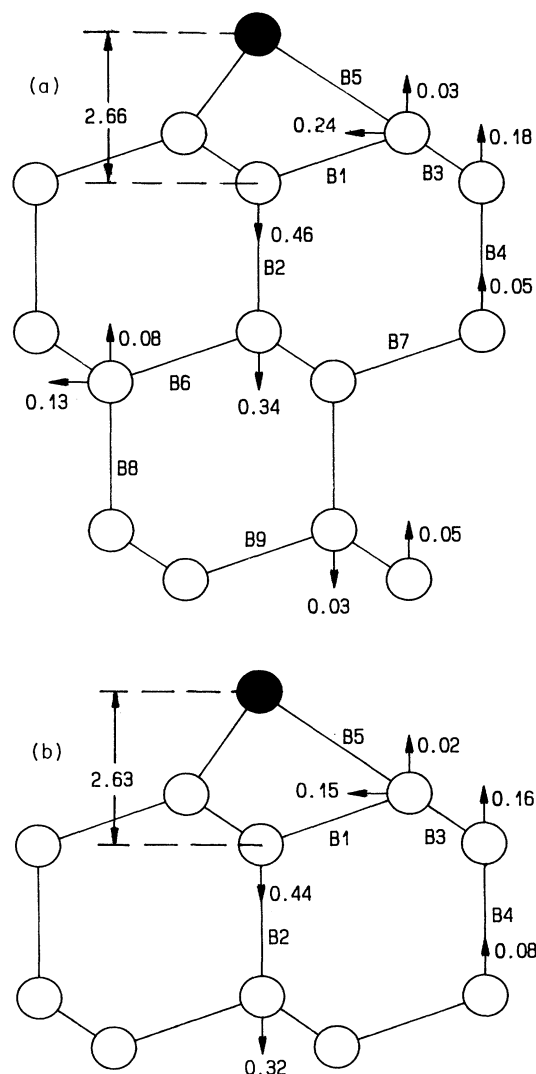


FIG. 4. Side view of the T_4 model of the Si(111)($\sqrt{3}\times\sqrt{3}$)R30°-Al surface. Solid circles represent the Al atoms and open circles the Si atoms. Arrows and numbers nearby are direction and quantity of the deviations (in Å) from the bulk positions, respectively. (a) Results of QKLEED. $B_1=2.35$ Å, $B_2=2.23$ Å, $B_3=2.43$ Å, $B_4=2.48$ Å, $B_5=2.41$ Å. (b) Results of DLEED.³⁷ $B_1=2.41$ Å, $B_2=2.23$ Å, $B_3=2.38$ Å, $B_4=2.43$ Å, $B_5=2.49$ Å.

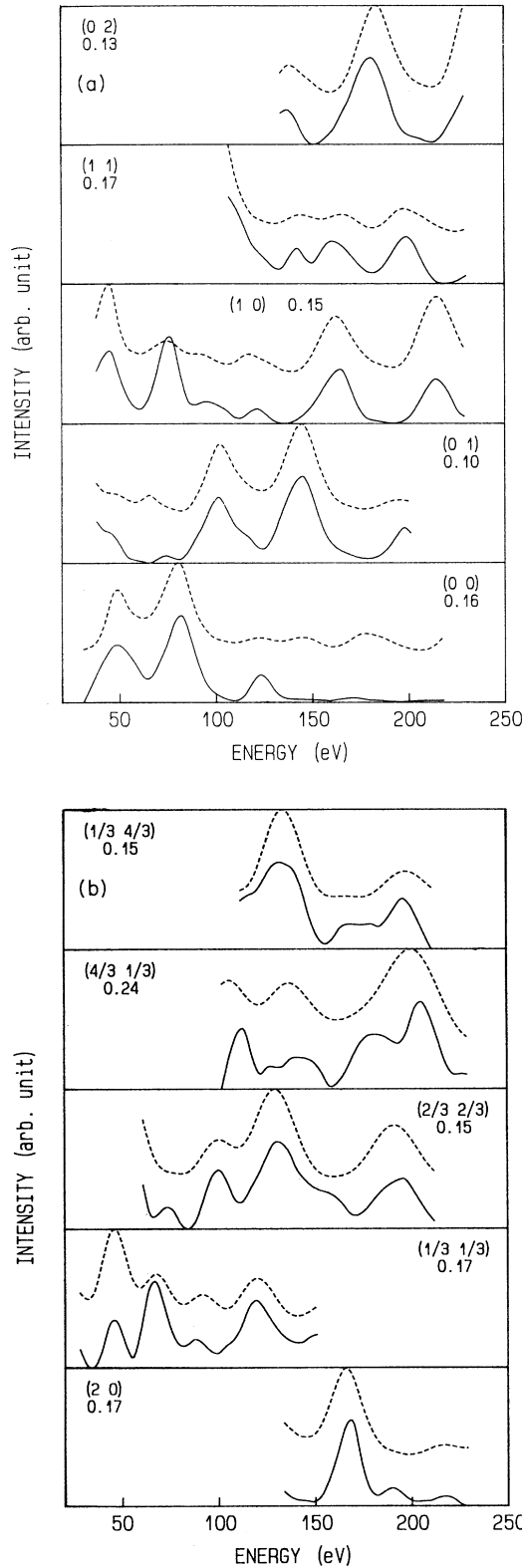


FIG. 5. Comparison of the QKLEED spectra (dashed) of the structure shown in Fig. 4(a) with the CMTA curves (solid) of the $\text{Si}(111)(\sqrt{3} \times \sqrt{3})R30^\circ\text{-Al}$ surface. The beam indices and r factors are shown in the boxes. The total R_{vht} of ten beams is 0.158.

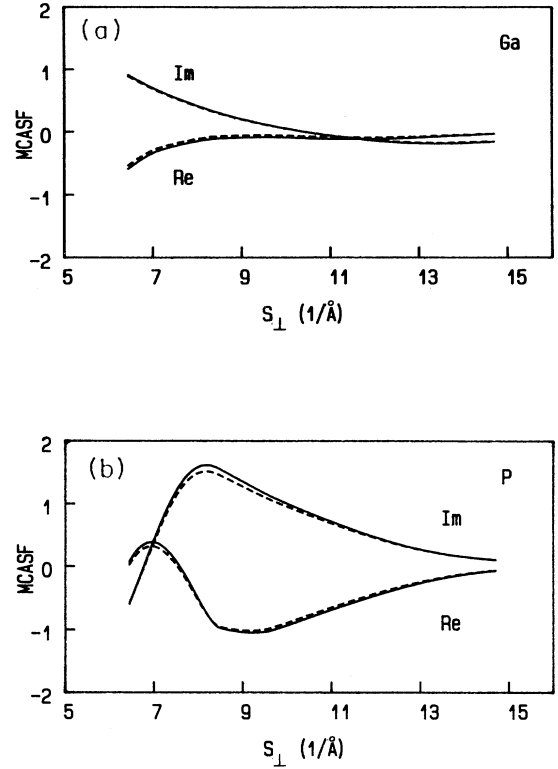


FIG. 6. Comparison of two sets of MCASF's of the (0,0) beam of the $\text{GaP}(111)(1 \times 1)$ surface. The solid-curve set involves the (θ, ϕ) 's of $(0^\circ, 0^\circ)$, $(4^\circ, 10^\circ)$, $(5^\circ, 40^\circ)$, $(8^\circ, 30^\circ)$, $(10^\circ, 0^\circ)$, $(12^\circ, 60^\circ)$, $(15^\circ, 30^\circ)$, $(18^\circ, 15^\circ)$, and $(20^\circ, 50^\circ)$, while those of the dashed-curve set are $(3^\circ, 55^\circ)$, $(6^\circ, 10^\circ)$, $(9^\circ, 30^\circ)$, $(14^\circ, 45^\circ)$, $(17^\circ, 20^\circ)$, $(19^\circ, 36^\circ)$, and $(21^\circ, 15^\circ)$. (a) Results of Ga atoms. (b) Results of P atoms.

B. An alternative to the MCASF

Of course, MCASF is not the only treatment of the effective scattering factors. Actually, one may fit an experimental CMTA curve with the CMTA of a set of QKLEED curves that have the same (θ, ϕ) 's as those involved in the experimental CMTA curve and are calculated with the use of the atomic scattering factor of the constituent atoms of the surface.²⁷ We call the CMTA of a set of QKLEED curves the CMTA-QKLEED. This treatment has been tested on the same $\text{GaP}(111)(1 \times 1)$ surface of Sec. IV. Compared with QKLEED curves of Fig. 2, the CMTA-QKLEED's of all six beams give a total R_{vht} of 0.10.³⁰ That means both of the approaches of the effective scattering factors can be used. However, obviously, the CMTA-QKLEED approach is about ten times more time consuming than the other one.

C. Avoiding local minima of the r factor

Being trapped by local minima is a common serious problem in parameter optimizations if many parameters are involved. Moreover, the complexity of DLEED calculations makes it even worse, thus at present no general strategy exists in LEED.⁴ Now the situation is different.

The QKLEED calculations are so simple that with a personal computer of 80386 we can calculate ten QKLEED curves of a Si(111)(7×7) structural model in a few seconds. As a result, many optimization procedures⁴⁴ can be adopted. For example, we have been using the simulated annealing⁴⁴ in conjunction with other procedures very successfully.^{30,43}

D. The R_{vht} level of a correct model

With the incorporation of optimization procedures into surface structure determinations, it becomes clear that a structural model with a R_{vht} of 0.2 or larger should not be claimed as the final solution of a surface structure. For instance, after optimization the R_{vht} of the H_3 model (wrong, of course) of Si(111)($\sqrt{3} \times \sqrt{3}$)R 30°-Al can be as low as 0.21,³⁰ and for the Si(111)($\sqrt{3} \times \sqrt{3}$)R 30°-Ag as well as Si(111)(7×7) surfaces similarly low or even lower R_{vht} had occurred for wrong models.³⁰ However, for complex surfaces such as those with DLEED calculations it is very difficult to find a model that can give a R_{vht} lower than 0.2. This fact emphasizes once more the importance of introducing the QKLEED/CMTA method into surface crystallography.

E. Where some old CMTA work failed

The failure of some old CMTA work was as important as the idea of CMTA for the QKLEED/CMTA. In short, in some work only CMTA curves of the (0,0) beam were used, which very often contains noticeable residual peaks of multiple scattering, as we have seen in Fig. 3. In some other work, the I-E spectra were distributed either in a small area (especially for ϕ) or not randomly enough in the $\theta\phi$ space. Some others failed to treat correctly the influence of the zero-angle scattering. Finally, none of them solved the effective scattering factors properly in studying surfaces consisting of two different atoms.

VII. SUMMARY

Based on the idea of CMTA of Lagally and co-workers, and awaking to the fact pointed out by Pendry that there are some residual influences in the CMTA curves coming mainly from the zero-angle scattering, we have proposed the QKLEED/CMTA method for surface structure determinations. The method includes the following.

On the experimental side, to get CMTA curves containing the lowest multiple scattering influence, according to the experimental design proposed in this work, 5–10 I-E spectra for each beam is enough, provided that the incidence geometries, i.e., (θ, ϕ)'s of these spectra, occupy as large an area as possible and are distributed randomly (evenly) in the $\theta\phi$ space.

On the QKLEED calculation side, the general lowering (raising) of inner potential, the reducing of intensities, and the increasing of peak widths caused by the zero-angle scattering are taken into account in such a way that they have essentially no influence on the attainment of correct surface structures. Meanwhile, to make the method applicable to surfaces consisting of more than one element, the MCASF is introduced as the effective scattering factor.

For parameter optimization, we have adopted a very powerful procedure, i.e., simulated annealing together with other useful procedures.

The validity of the whole QKLEED/CMTA method has passed careful tests from every possible direction we could think of, and its capability of attaining the right surface structures has been demonstrated on the Cu(001)(1×1), Si(111)($\sqrt{3} \times \sqrt{3}$)R 30°-Al, and Si(111)($\sqrt{3} \times \sqrt{3}$)R 30°-Ag surfaces.

ACKNOWLEDGMENTS

We thank Dr. M. A. Van Hove for providing the LEED package from which the phase-shift data were taken. This work was supported by the National Natural Science Foundation of China and the Doctoral Program Foundation of Institute of Higher Education of China

¹J. B. Pendry, *Low-Energy Electron Diffraction* (Academic, New York, 1974).

²M. A. Van Hove and S. Y. Tong, *Surface Crystallography by LEED* (Springer-Verlag, Berlin, 1979).

³F. Jona, J. A. Strozier, Jr., and W. S. Yang, *Rep. Prog. Phys.* **45**, 527 (1982).

⁴M. A. Van Hove, W. H. Wienberg, and C.-M. Chan, *Low-Energy Electron Diffraction* (Springer-Verlag, Berlin, 1986).

⁵P. J. Rous, in *The Structure of Surfaces III*, edited by S. Y. Tong *et al.* (Springer-Verlag, Berlin, 1991).

⁶S. Y. Tong, H. Huang, C. M. Wei, W. E. Packard, F. K. Men, G. Glander, and M. B. Webb, *J. Vac. Sci. Technol. A* **6**, 615 (1988).

⁷M. G. Lagally, T. C. Ngoc, and M. B. Webb, *Phys. Rev. Lett.* **26**, 1557 (1971).

⁸M. G. Lagally, T. C. Ngoc, and M. B. Webb, *J. Vac. Sci. Tech-*

nol. **9**, 645 (1972).

⁹J. B. Pendry, *J. Phys. C* **5**, 2567 (1972).

¹⁰C. B. Duke and D. L. Smith, *Phys. Rev. B* **5**, 4730 (1972).

¹¹D. T. Quinto and W. D. Robertson, *Surf. Sci.* **34**, 501 (1973).

¹²T. C. Ngoc, M. G. Lagally, and M. B. Webb, *Surf. Sci.* **35**, 117 (1973).

¹³J. M. Burkstrand, G. G. Kleiman, and F. J. Arlinghaus, *Surf. Sci.* **46**, 43 (1974).

¹⁴L. McDonnell, D. P. Woodruff, and K. A. R. Mitchell, *Surf. Sci.* **45**, 1 (1975).

¹⁵J. C. Buchholz, G.-C. Wang, and M. G. Lagally, *Surf. Sci.* **49**, 508 (1975).

¹⁶G. G. Kleiman and J. M. Burkstrand, *Surf. Sci.* **50**, 493 (1975).

¹⁷M. G. Lagally, J. C. Buchholz, and G.-C. Wang, *J. Vac. Sci. Technol.* **12**, 213 (1975).

¹⁸W. N. Unertl and H. V. Thapliyal, *J. Vac. Sci. Technol.* **12**,

- 263 (1975).
- ¹⁹W. N. Unertl and M. B. Webb, *Surf. Sci.* **59**, 373 (1976).
- ²⁰S. J. White and D. P. Woodruff, *Surf. Sci.* **63**, 254 (1977).
- ²¹S. J. White and D. P. Woodruff, *Surf. Sci.* **64**, 131 (1977).
- ²²A. Kahn, G. Cisneros, M. Bonn, and P. Mark, *Surf. Sci.* **71**, 387 (1978).
- ²³A. Kahn, E. So, P. Mark, and C. B. Duke, *J. Vac. Sci. Technol.* **15**, 580 (1978).
- ²⁴A. Kahn, E. So, P. Mark, C. B. Duke, and R. J. Meyer, *J. Vac. Sci. Technol.* **15**, 1223 (1978).
- ²⁵T. D. Poppendieck, T. C. Ngoc, and M. B. Webb, *Surf. Sci.* **75**, 287 (1978).
- ²⁶J. H. Onuferko and D. P. Woodruff, *Surf. Sci.* **91**, 400 (1980).
- ²⁷Y. Terada, T. Yoshizuka, K. Oura, and T. Hanawa, *Surf. Sci.* **114**, 65 (1982).
- ²⁸W. S. Yang and R. G. Zhao, *Phys. Rev. B* **30**, 6016 (1984).
- ²⁹R. G. Zhao and W. S. Yang, *Phys. Rev. B* **33**, 6780 (1986); R. G. Zhao, J. F. Jia, Y. F. Li, and W. S. Yang, in *The Structure of Surfaces III* (Ref. 5), p. 517.
- ³⁰J. F. Jia, Doctoral thesis, Peking University, 1992.
- ³¹M. A. Van Hove, S. Y. Tong, and M. H. Elconin, *Surf. Sci.* **64**, 85 (1977).
- ³²H. L. Davis and J. R. Noonan, *J. Vac. Sci. Technol.* **20**, 842 (1982).
- ³³W. S. Yang, F. Jona, and P. M. Marcus, *Phys. Rev. B* **28**, 7337 (1985).
- ³⁴J. J. Lander and J. Morrison, *Surf. Sci.* **2**, 553 (1964).
- ³⁵J. E. Northrup, *Phys. Rev. Lett.* **53**, 683 (1984).
- ³⁶J. M. Nicholls, B. Reichl, and J. E. Northrup, *Phys. Rev. B* **35**, 4137 (1987).
- ³⁷R. J. Hamers and J. J. Demuth, *Phys. Rev. Lett.* **60**, 2527 (1988).
- ³⁸H. Huang, S. Y. Tong, W. S. Yang, H. D. Shih, and F. Jona, *Phys. Rev. B* **42**, 7483 (1990).
- ³⁹E. Vlieg, E. Fontes, and J. K. Patel, *Phys. Rev. B* **43**, 7185 (1991).
- ⁴⁰T. Takahashi, S. Nakatani, N. Okamoto, T. Ishikawa, and S. Kikuta, *Surf. Sci.* **242**, 54 (1991).
- ⁴¹M. Katayama, R. S. Williams, M. Kato, E. Nomura, and M. Aono, *Phys. Rev. Lett.* **66**, 2762 (1991).
- ⁴²Y. G. Ding, C. T. Chan, and K. M. Ho, *Phys. Rev. Lett.* **67**, 1454 (1991).
- ⁴³J. F. Jia, R. G. Zhao, and W. S. Yang, *Phys. Rev. B* **48**, 18109 (1993).
- ⁴⁴W. H. Press, B. P. Flannery, S. A. Teukolsky, and W. T. Vetterling, *Numerical Recipes* (Cambridge University Press, Cambridge, 1986); S. Saito and A. Oshiyama, *Phys. Rev. Lett.* **66**, 2637 (1991).